14th European Signal Processing Conference (EUSIPCO 2006), Florence, Italy, September 4-8, 2006, copyright by EURASIP

COHERENCE ESTIMATION BETWEEN EEG SIGNALS USING MULTIPLE WINDOW TIME-FREQUENCY ANALYSIS COMPARED TO GAUSSIAN KERNELS

Johan Sandberg and Maria Hansson

Mathematical Statistics, Centre for Mathematical Sciences, Lund University.
Address: Box 118, SE-221 00 Lund, Sweden. Phone: + (46) 46 22 285 50. Fax: +46 46 22 246 23.
Email: sandberg@maths.lth.se, mh@maths.lth.se. Web: www.maths.lth.se/matstat

ABSTRACT

It is believed that neural activity evoked by cognitive tasks is spatially correlated in certain frequency bands. The electroencephalogram (EEG) is highly affected by noise of large amplitude which calls for sophisticated time local coherence estimation methods.

In this paper we investigate different approaches to estimate time local coherence between two real valued signals. Our results indicate that the method using two dimensional Gaussian kernels has a slightly better average SNR compared to the multiple window approach. On the other hand, the multiple window approach has a more narrow SNR distribution and seems to perform better in the worst case.

1. INTRODUCTION

The electroencephalogram technique (EEG) visualizes the brain activity to a low cost and in a simple and non-invasive way. Despite the last three decades of development of brain mapping techniques, EEG attracts attention in numerous research disciplines and in clinical practice. One reason for this is the method's extraordinary temporal resolution. And since neural communication occurs through potentials, the EEG is a low-level, natural mean for monitoring the activity of the brain.

The spatially synchronized activity of the cortical areas interacts while performing various cognitive tasks. It is hypothesized that when a particular task is carried out, the involved cortical areas attain synchronized activity within specific frequency bands, [1]. Many analyses of synchronized activity and neural cooperation are performed in the frequency domain by calculating the coherence between the electrodes. Recent publications indicate that diagnose of certain disorders and conditions, e.g. Alzheimer's disease and mild cognitive impairment, [2, 3], may be aided by studies of synchronized activity. It has been observed that the pattern of active cortical areas, or the degree of synchronization between particular areas, differs between healthy individuals and individuals with disorders. Besides using spatial synchronization in the EEG as a diagnostic aid, it is also used in the investigation of language, [4, 5], where differences in brain activity during processing of words from various classes (e.g. concrete vs. abstract nouns) have been found. Recent studies has also expanded long-standing assumptions on brain oscillations and cognitive function, especially memory processes, [6].

The frequency content is usually estimated by successively averaged sub-spectra from different time epochs. Events of short duration will be difficult to detect and the onset and offset time of those events will be misinterpreted. Such transient frequency changes are often of great interest. Event-related changes in the spectrogram are of interest in, e.g., cognitive studies, [7].

Cross-spectral analysis of non-stationary processes has been done, e.g. in [8], where it is shown that the estimate from the smoothed short-time Fourier transform (STFT) (equivalent to multiple window STFT) is the most appropriate. Non-parametric coherence analysis of non-stationary signals is done, e.g., in [9, 10, 11].

The coherence, $\rho^2_{xy}(f)$, between two real valued signals $x(t)$ and $y(t)$ is a function of frequency that measures the proportion of energy in one signal at one frequency that can be explained by a linear filter transformation of the other signal. It is defined:

$$\rho^2_{xy}(f) \equiv \frac{\left|R_{xy}(f)\right|^2}{R_x(f)R_y(f)} \quad ,$$

where $R_{xy}(f)$ is the cross spectral density and $R_x(f)$ and $R_y(f)$ are spectral densities. In the case of time discrete signals, $x(t)$, $y(t)$, $t = 1, \ldots, n$, it seems natural to take $\hat{\rho}^2_{xy} = |\hat{R}_{xy}(f)|/\hat{R}_x(f)\hat{R}_y(f)$ as an estimate. However, this estimate is identical to 1, if the spectral densities is estimated with the periodogram and the cross spectral density is estimated with the Fourier transform of the estimated cross covariance function: $\mathscr{F}(\hat{r}_{xy}(\tau)) = \mathscr{F}\left(\frac{1}{N}\sum_t x(t)y(t+\tau)\right) = \frac{1}{n}\mathscr{F}(x(t))\mathscr{F}(y(t))^*$, where the asterisk denotes complex conjugate. This well known result may not come as a surprise since we have tried to estimate n different estimators (n different values of f in $\hat{\rho}^2_{xy}(f)$) out of n different values of $x(t)$ and $y(t)$. Different ways of smoothing the periodogram, e.g. averaging nearby frequencies with a kernel, will solve this problem.

For non-stationary signals, we are interested in time local coherence. This could be achieved by the use of a two dimensional time frequency kernel, as described in Section 2, or by the use of multiple time windows as described in Section 3. The methods are compared on simulated data which share some important features with real EEG. We evaluate them using signal to noise ratio. All of this is presented in Section 4. The same methods are applied to real EEG data in Section 5 and finally some conclusions are drawn in Section 6.

2. COHERENCE ESTIMATION USING GAUSSIAN KERNELS

We are interested in estimating a time local coherence function, $\rho_{X,Y}(t_0, f_0)$, at time t_0 and frequency f_0 of two non-stationary real valued signals $x(t)$ and $y(t)$. Using the approach of Gaussian kernels, we first compute local Fourier transforms, $X_H(t, f)$ and $Y_H(t, f)$, using a Hanning window,

H, as a frame. The length of the Hanning window is of course crucial, since it determines the balance between time and frequency resolution of $X_H(t,f)$ and $Y_H(t,f)$.

We need a whole set of time frequency estimates in a surrounding of (t_0, f_0) to be able to estimate a local coherence. The selection of this set is made by a kernel, $K_{t_0,f_0}(t,f)$, which has its maximum value at (t_0, f_0). A trade-off must be made between low variance (many time frequency estimates, i.e. a wide kernel) and low bias (few time frequency estimates to ensure a precise time frequency resolution). In this paper only Gaussian kernels are considered. They can be written on the form:

$$K_{t_0,f_0}(t,f) = \frac{1}{\sqrt{2\pi}\sigma_t^2} e^{-\frac{(t-t_0)^2}{2\sigma_t^2}} \frac{1}{\sqrt{2\pi}\sigma_f^2} e^{-\frac{(f-f_0)^2}{2\sigma_f^2}} \quad .$$

Using a particular kernel, K, the local coherence, $\rho_{X,Y}(t_0,f_0)$, can be estimated:

$$\hat{\rho}^K_{X,Y}(t_0,f_0) = \frac{|S^K_{XY}(t_0,f_0)|}{\sqrt{S^K_{XX}(t_0,f_0)S^K_{YY}(t_0,f_0)}} \quad ,$$

where $S_{XY}(t_0,f_0)$, $S_{XX}(t_0,f_0)$ and $S_{YY}(t_0,f_0)$ are double sums of time frequency estimates weighted with the kernel:

$$\begin{aligned} S^K_{XY}(t_0,f_0) &= \sum_t \sum_f K_{t_0,f_0}(t,f) X_H(t,f) Y_H(t,f)^* \\ S^K_{XX}(t_0,f_0) &= \sum_t \sum_f K_{t_0,f_0}(t,f) X_H(t,f) X_H(t,f)^* \\ S^K_{YY}(t_0,f_0) &= \sum_t \sum_f K_{t_0,f_0}(t,f) Y_H(t,f) Y_H(t,f)^* \quad , \end{aligned}$$

where complex conjugate is denoted with an asterisk.

3. COHERENCE ESTIMATION USING MULTIPLE WINDOWS

The key to estimate coherence is to have many uncorrelated time frequency estimates at approximately the same time and frequency. In this approach we make use of multiple windows (MW), which are windows located close to each other within a single frame. They are designed to have low covariance even though they overlap.

To estimate the local coherence function, $\rho_{X,Y}(t_0,f_0)$, between the real valued signals $x(t)$ and $y(t)$ we first form a frame centred at t_0 with N (overlapping) multiple windows, $w_{i,t_0}(t)$, $i = 1, \ldots, N$, as schematically displayed in Figure 1. We compute the Fourier transforms, $X_{i,t_0}(f)$ and $Y_{i,t_0}(f)$ of each segment $x(t)w_{i,t_0}(t)$ for $i = 1, \ldots, N$, and $y(t)w_{i,t_0}(t)$ for $i = 1, \ldots, N$. The local coherence function, $\rho_{X,Y}(t_0,f_0)$ is then estimated:

$$\hat{\rho}^W_{X,Y}(t_0,f_0) = \frac{|S^W_{XY}(t_0,f_0)|}{\sqrt{S^W_{XX}(t_0,f_0)S^W_{YY}(t_0,f_0)}} \quad ,$$

where the superscript indicates that the sums, S^W_{XY}, S^W_{XX} and S^W_{YY} are depending on a set of multiple windows, $\{w_1, \ldots, w_N\}$:

$$\begin{aligned} S^W_{XY}(t_0,f_0) &= \sum_{i=1}^N X_{i,t_0}(f_0) Y_{i,t_0}(f_0)^* \\ S^W_{XX}(t_0,f_0) &= \sum_{i=1}^N X_{i,t_0}(f_0) X_{i,t_0}(f_0)^* \\ S^W_{YY}(t_0,f_0) &= \sum_{i=1}^N Y_{i,t_0}(f_0) Y_{i,t_0}(f_0)^* \quad . \end{aligned}$$

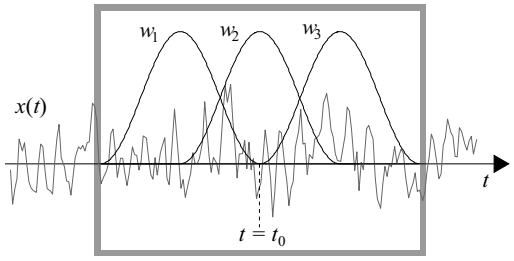

Moving frame

Figure 1: Example of multiple windows, w_i, $i = 1, \ldots, 3$. A frequency estimate is computed within each window and then averaged to reduce variance. Even though the multiple windows overlap, they give almost uncorrelated frequency estimates for the kinds of processes they are designed for. The picture shows Welch windows, see Section 3.1.

It is important that the correlation between the N windowed periodogram, $X_{i,t_0}(f)$, $i = 1, \ldots, N$, is small for all f (and the same goes for $Y_{i,t_0}(f)$). When the multiple windows are appropriate chosen, with respect to the properties of the stochastic process, this can be achieved even if the multiple windows is overlapping within one frame. There are different ways to achieve small correlation of different sub-spectra. In the following subsections three different multiple windows are described.

3.1 Welch multiple windows

In the WOSA algorithm, [12], the overlap of the sequences can be varied but it has been shown that 50% overlap, as used in this paper, is a good choice. The windows are then defined as

$$w_i = [\underbrace{0, \ldots, 0}_{(i-1)\frac{M_w}{2}}, w^T, \overbrace{0, \ldots, 0}^{M-(i+1)\frac{M_w}{2}}]^T; \quad i = 1, \ldots, N \quad ,$$

where w is a Hanning window (of length M_w) and the number of windows N is the largest integer where $N \leq \frac{2M}{M_w} - 1$. With these windows the data samples x are divided into overlapping sequences $x\left((t-1)\frac{M_w}{2}\right), \ldots, x\left((t+1)\frac{M_w}{2} - 1\right)$ and each sequence is windowed with the same data window. It is assumed that the random samples of data give N uncorrelated sub-spectra which are then averaged. An example of Welch multiple windows is shown in Figure 1.

3.2 Peak matched multiple windows (PM MW)

An example of the Peak Matched Multiple Windows (PM MW), [13], is shown in Figure 2. The PM MW are designed

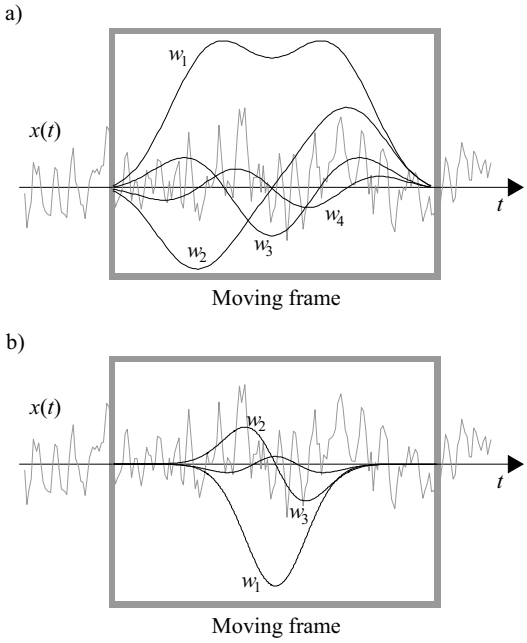

Figure 2: Example of multiple windows. Peak matched multiple windows in a) and local stationary process optimal multiple windows in b).

to give small correlation between sub-spectra when the spectrum of the random process includes peaks and notches, i.e., spectra with large dynamics. The windows are given by the solution of the generalized eigenvalue problem

$$\mathbf{R}_B\mathbf{q}_i = \lambda_i\mathbf{R}_Z\mathbf{q}_i, \quad i = 1, \ldots, L \quad ,$$

where the eigenvalues are ordered in decreasing magnitude, $\lambda_1 \geq \lambda_2 \geq \ldots \geq \lambda_L$. The $(L \times L)$ Toeplitz covariance matrix $\mathbf{R}_B$ has the elements $r_B(l) = r_{x_d}(l) * r_{box}(l)$, $0 \leq |l| \leq L-1$, where $r_{x_d}(l)$ is the covariance function of a desired peaked spectrum process $x_d(t)$ and $*$ denotes the convolution operator.

3.3 Locally stationary process optimal multiple windows (LSP OPT MW)

A locally stationary process (LSP) has a covariance function determined by two functions,

$$r_x(t,s) = q\big(\frac{t+s}{2}\big) \cdot r(t-s) \quad ,$$

where $q(\tau) = e^{-\tau^2/2}$ is a fix Gaussian function and $r(\tau) = e^{-\frac{c}{4}\tau^2/2}$ is a variable Gaussian function. The function, $r_x(t,s)$, is a covariance if and only if $c \geq 1$. The expected ambiguity function of a locally stationary process is separable (rank one),

$$A_x(\theta,\tau) = Q(\theta)r(\tau).$$

The optimal kernel is

$$\begin{aligned}\phi_{opt}(\theta,\tau) &= \frac{|Q(\theta)|^2|r(\tau)|^2}{|Q(\theta)|^2|r(\tau)|^2 + (\mathscr{F}|r|^2)(\theta)(\mathscr{F}^{-1}|Q|^2)(\tau)} \\ &= \frac{1}{1 + c^{-1/2}e^{(1-\frac{1}{c})\theta^2 + \frac{c-1}{4}\tau^2}},\end{aligned}$$

[14]. The optimal multiple windows for a time-variable process are obtained as the eigenvectors of a rotated time-lag estimation kernel, [15]. Figure 2 shows an example of LSP OPT MW.

4. RESULTS ON SIMULATED DATA

4.1 The data

The simulated data is inspired by known properties of EEG. Interesting components of the EEG is often hidden by larger components with slightly higher or lower frequency making time frequency analyze difficult. Spikes and high frequency noise are often present.

The coherence estimation methods are evaluated on pairs of twenty seconds long simulated signals, $x(t)$ and $y(t)$, sampled at 256 Hz. The two signals are composed of uncorrelated components plus a common component of smaller amplitude. The components of $x(t)$ are:

- A one second long AR(2) process with frequency 15 Hz, centred at $t = 10$ s. It is smoothly raised and lowered with a one second long Hanning window. Its mean energy is 0.25. This is the only component identical for both $x(t)$ and $y(t)$.
- A one second long AR(2) process with frequency $15+\delta$ Hz and mean energy equal to 1. It is centred at $t = 10$ s and smoothly raised and lowered with a one second long Hanning window.
- A spike at $t = 9$ s.
- White Gaussian noise with mean energy 0.05.

The signal $y(t)$ is simulated in a similar manner:

- A one second long AR(2) process with frequency 15 Hz, centred at $t = 10$ s. It is smoothly raised and lowered with a one second long Hanning window. Its mean energy is 0.25. This is the only component identical for both $x(t)$ and $y(t)$.
- A one second long AR(2) process with frequency $15-\delta$ Hz and mean energy equal to 1. It is centred at $t = 10$ s and smoothly raised and lowered with a one second long Hanning window.
- A spike at $t = 11$ s.
- White Gaussian noise with mean energy 0.05.

A realization of $x(t)$ and $y(t)$ are presented in the time frequency plane in Figure 3. The target for our coherence estimation methods is to find the one second long coherence at frequency 15 Hz even though the signals have large non correlated energy content at $15-\delta$ and $15+\delta$ and also spikes at $t = 9$ and $t = 11$ s, respectively. Next section will discuss how to evaluate the time-frequency coherence estimates produced by the different methods.

4.2 Evaluation method

We expect the coherence of $x(t)$ and $y(t)$ to be zero everywhere except between $t = 9.5$ and $t = 10.5$ s at frequency 15 Hz. Since it is reasonable to believe that small coherence values are due to noise we apply a threshold level at the 90%-quantile, leaving only ten percentages unaffected.

We define the signal to noise ratio (SNR) as the mean estimated coherence in the time frequency area $t = 10 \pm 0.5$ s, $f = 15 \pm 1.5$ Hz divided with the mean estimated coherence in a larger surrounding time frequency area ($t = 10 \pm 2.5$ s, $f = 15 \pm 4$ Hz). By simulating many pairs of $x(t)$ and $y(t)$ we

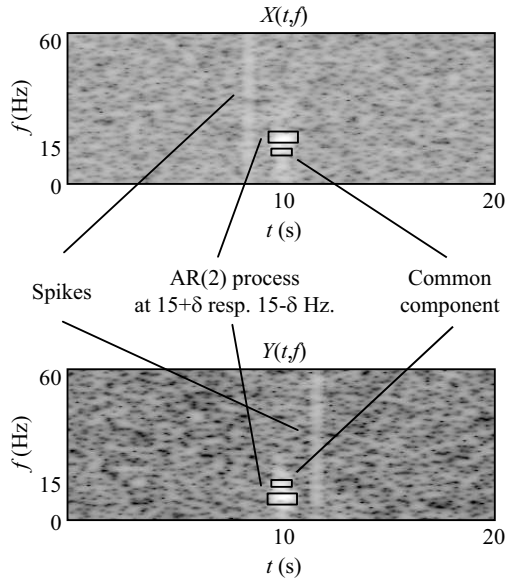

Figure 3: The simulated signals, $x(t)$ and $y(t)$, is a sum of four different components (white noise, spikes and two AR-process of which one is the same in both $x(t)$ and $y(t)$). They are only correlated at $9.5 < t < 10.5$ (s) and $f = 15$ (Hz).

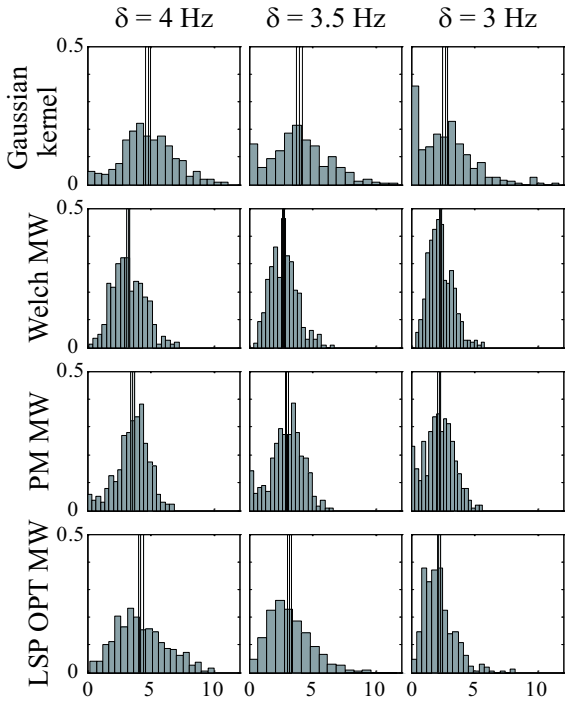

Figure 4: The histograms shows the distribution of SNR for four different methods and three different values of δ. Mean and its approximately 95% confidence interval is indicated. Number of simulations is 400.

can get a picture of different coherence estimation methods' SNR distribution.

4.3 Results

Modifying the composition of $x(t)$ and $y(t)$ largely affects the optimal adjustments of the coherence estimation methods. The parameter δ, which is the distance, in Hz, between the correlated component at 15 Hz and the two disturbing AR(2) processes at $15 \pm \delta$ Hz, has greatest impact on the performance of different methods.

Figure 4 shows histograms of the performance of four different coherence estimation methods and three different values of δ. The performance is measured using SNR as described previously. The evaluated methods are: (a) a Gaussian kernel (Hanning window length was 1 second, $\sigma_f = 1.25$, and $\sigma_t = 0.469$.), (b) the Welch MW (frame length was 1 second, $N = 4$), (c) the PM MW (frame length two seconds, $N = 4$) and (d) the LSP OPT MW (frame length two seconds, $N = 5$). Note that even though the Gaussian kernel method has slightly higher average SNR for all three values of δ, it performs very badly more often than the others for low values of δ. Taking this important fact into account, one might say that the MW methods sometimes are slightly superior to the method using Gaussian kernels.

5. RESULTS ON REAL EEG DATA

To show the performance for real-data, EEG was recorded from a healthy subject presented to a 9-Hz flickering light (Grass Photic stimulator Model PS22C). The subject was supine with closed eyes on a bed in a silent laboratory. Ambient light was dimmed. A flickering light was flashed at the subject from a distance of approximately 1 m during one second. The sampling rate was 256 Hz. Figure 5 shows the estimated coherence between electrodes placed at F3 and P4 according to the international 10-20 system. Coherence estimates are made with the same methods as evaluated with simulated data in Section 4, but a few parameters had to be adjusted. The estimates were made using (a) a Gaussian kernel (Hanning window length was 1 second, $\sigma_f = 0.625$, and $\sigma_t = 0.469$.), (b) the Welch MW (frame length was two seconds, $N = 4$), (c) the PM MW (frame length two seconds, $N = 4$) and (d) the LSP OPT MW (frame length two seconds, $N = 5$). All estimates shows a particularly high coherence at 9 Hz when the light was flickering, indicating synchronized cortical activity. However, there is also high coherence at some other time frequency areas.

6. CONCLUSIONS

The problem of local coherence estimation is very difficult and different strategies will have different advantages and drawbacks. Furthermore, it is not trivial to develop a reasonable measurement by which different methods can be compared. Using SNR as described above, indicates that estimation techniques using MW are interesting alternatives to the Gaussian kernel approach, especially when the correlated components are masked by larger components closely located in time and frequency.

7. ACKNOWLEDGMENTS

This work was supported by the Swedish Research Council.

REFERENCES

[1] P. L. Nunez, "Toward a quantitative description of large-scale neocortical dynamic function and EEG",

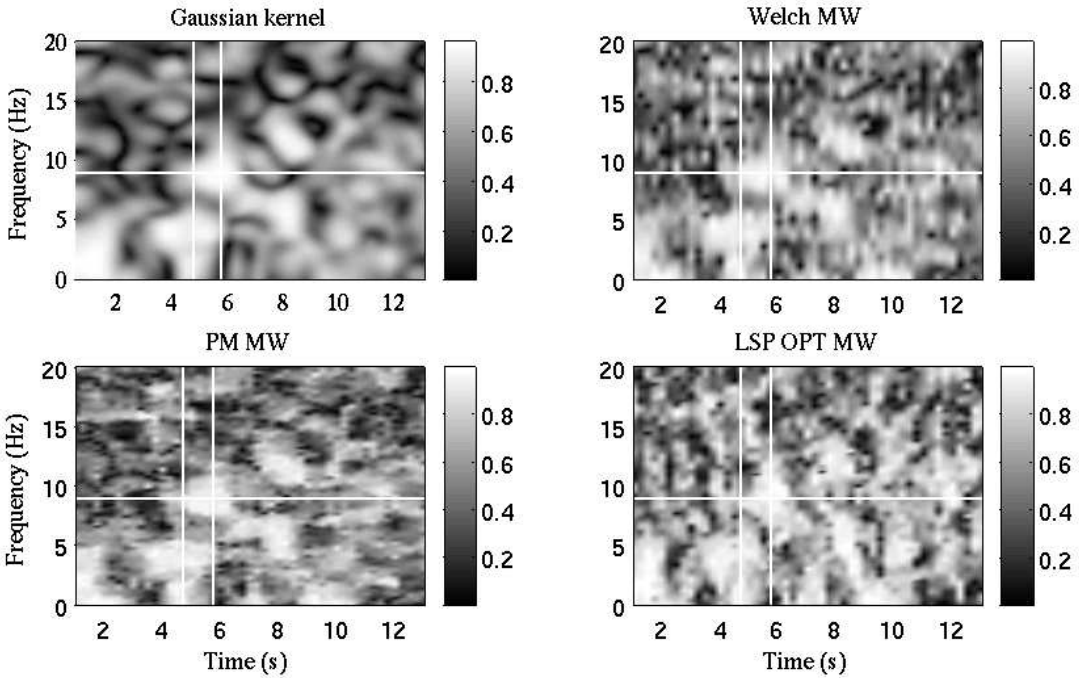

Figure 5: Coherence between channel F3 and P4 estimated using four different methods: the Gaussian kernel method, the Welch MW, PM MW and LSP OPT MW. At $t = 4.7$ the subject is presented to a 9 Hz flickering light which last for one second.

Behavioral and Brain Sciences, vol. 23, pp. 371–437, 2000.

[2] T. Locatelli, M. Cursi, D. Liberati, M. Franceschi, and G. Comi, "Eeg coherence in alzheimer's disease", *Electroencephalography and clinical Neurophysiology*, vol. 106, pp. 229–237, 1998.

[3] C. J. Stam, Y. van der Made, Y. A. L. Pijnenburg, and P. Scheltens, "Eeg synchronization in mild cognitive impairment and alzheimer's disease", *Acta Neurologica Scandinavica*, vol. 108, pp. 90–96, 2003.

[4] S. Weiss and H. M. Mueller, "The contribution of eeg coherence to the investigation of language", *Brain and Language*, vol. 85, pp. 325–343, 2003.

[5] P. Khader and F. Rösler, "Eeg power and coherence analysis of visually presented nouns and verbs reveals left frontal processing differences", *Neuroscience Letters*, vol. 354, pp. 111–114, 2004.

[6] M. J. Kahana, D. Seelig, and J. R. Madsen, "Theta returns", *Current opinion in Neurobiology*, vol. 11, pp. 739–744, 2001.

[7] Klimesch W, Doppelmayr M, Schimke H, and Ripper B, "Theta synchronization and alpha desynchronization in a memory task", *Psychophysiology*, vol. 34, pp. 169–176, 1997.

[8] L. B. White and B. Boashash, "Cross spectral analysis of nonstationary processes", *IEEE Trans. on Information Theory*, vol. 36, no. 4, pp. 830–835, 1990.

[9] G. Matz and F. Hlawatsch, "Time-frequency coherence analysis of non-stationary random processes", in *Proc of the 10th IEEE Workshop on Statistical Signal and Array Processing*. IEEE, 2000, pp. 554–558.

[10] K. Ansari-Asl, F. Wendling, J.J. Belanger, and L. Senhadji, "Comparison of two estimators of time-frequency interdependencies between nonstationary signals: application to epileptic eeg", in *Proc. of the 26th Annual Int. Conf of the IEEE Engineering in Medicine and Biology Society*, San Francisco, USA, Sept 1-5 2004, IEEE, pp. 263–266.

[11] D. J. Thomson, "Spectrum estimation and harmonic analysis", *Proc. of the IEEE*, vol. 70, no. 9, pp. 1055–1096, Sept 1982.

[12] P. D. Welch, "The use of fast fourier transform for the estimation of power spectra: A method based on time averaging over short, modified periodograms", *IEEE Trans. on Audio Electroacoustics*, vol. AU-15, no. 2, pp. 70–73, June 1967.

[13] M. Hansson and G. Salomonsson, "A multiple window method for estimation of peaked spectra", *IEEE Trans. on Signal Processing*, vol. 45, no. 3, pp. 778–781, March 1997.

[14] P. Wahlberg and M. Hansson, "Optimal time-frequency kernels for spectral estimation of locally stationary processes", in *IEEE Workshop on Statistical Signal Processing*, St. Louis, USA, 2003.

[15] M. Hansson and P. Wahlberg, "Optimal multiple window time-frequency analysis of locally stationary processes", in *European Signal Processing Conference (EUSIPCO)*, Vienna, Austria, 2004.